RefOnce: Distilling References into a Prototype Memory for Referring Camouflaged Object Detection

Yu-Huan Wu 1,2 Zi-Xuan Zhu 1 Yan Wang 2 Liangli Zhen 2 Deng-Ping Fan 1† VCIP, CS, Nankai University 2 IHPC, A*STAR, Singapore

wyh.nku@gmail.com https://github.com/yuhuan-wu/RefOnce

Abstract

Referring Camouflaged Object Detection (Ref-COD) segments specified camouflaged objects in a scene by leveraging a small set of referring images. Though effective, current systems adopt a dual-branch design that requires reference images at test time, which limits deployability and adds latency and data-collection burden. We introduce a Ref-COD framework that distills references into a class-prototype memory during training and synthesizes a reference vector at inference via a query-conditioned mixture of prototypes. Concretely, we maintain an EMA-updated prototype per category and predict mixture weights from the query to produce a guidance vector without any test-time references. To bridge the representation gap between reference statistics and camouflaged query features, we propose a bidirectional attention alignment module that adapts both the query features and the class representation. Thus, our approach yields a simple, efficient path to Ref-COD without mandatory references. We evaluate the proposed method on the large-scale R2C7K benchmark. Extensive experiments demonstrate competitive or superior performance of the proposed method compared with recent state-of-the-arts.

1. Introduction

Camouflaged object detection (COD) aims to segment targets that intentionally resemble their surroundings, which is a capability vital to many applications like medical imaging [6, 7, 45], industrial inspection [2], and crop pest monitoring [25]. Despite recent impressive advances [5, 8, 35], COD remains extremely challenging because camouflaged targets have very low visual contrast and their appearance cues are easily suppressed by cluttered backgrounds [31]. Intuitively, if we could observe the same category in cleaner, more salient conditions, such as reference images with distinct targets, the model could learn more stable, class-level

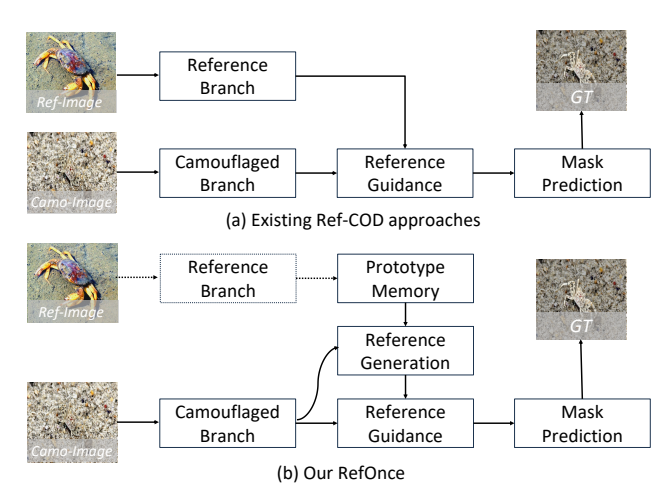


Figure 1. Comparison between (a) existing Ref-COD approaches [44, 56] and (b) our RefOnce framework. RefOnce retrieves the reference from the prototype memory to enable reference-free inference.

semantics and transfer them to ambiguous camouflaged scenes. This simple intuition naturally leads to Referring Camouflaged Object Detection (Ref-COD) [56], an intriguing and emerging task where a small set of reference images with salient targets guides the detection of the specified camouflaged object.

Recent pioneers of Ref-COD [44, 56] have demonstrated that introducing reference images with clear backgrounds significantly improves the discriminability of COD models. R2CNet [56] employs a dual-branch design: one branch extracts common representations from the reference images, while the other performs camouflaged segmentation under their modulation. Such designs successfully transform COD from blind searching into target-oriented detection, yielding strong quantitative gains and visually coherent masks. More advanced models like uncertainty-aware transformers [44] further enhance the guidance to camouflaged object features from references.

However, despite these successes, two core challenges remain. First, existing Ref-COD methods rely on a set of

[†]Corresponding Author: Deng-Ping Fan (fdp@nankai.edu.cn)

reference images of the same categories during inference to provide class-level guidance. However, in realistic deployment, this dependency is impractical because the camouflaged targets are visually ambiguous and category identification itself demands human efforts or external annotations. In other words, before the model can even segment the camouflaged object, one must first know its category to retrieve the corresponding reference images, a process that contradicts the goal of automatic detection. This challenge is further exacerbated by the scarcity of high-quality reference data and the privacy constraints in some application domains. Second, there exists a significant gap between the salient reference domain and the low-contrast camouflaged query domain, causing weak spatial alignment and degraded guidance transfer. Existing approaches mainly apply global affine modulation from reference features, which only weakly aligns spatial semantics and often causes overtransfer or misalignment. These issues motivate us to rethink the Ref-COD task: Can we distill the essential reference knowledge during training, enabling reference-free inference while simultaneously bridging the domain gap between reference and camouflaged features?

To address these challenges, we propose a novel Ref-COD framework RefOnce, which only relies on reference images during training. RefOnce is built upon two complementary ideas. First, to resolve the core deployment challenge, we design a class-prototype memory that stores category-level prototypes distilled from reference features during training, updated with an exponential moving average. During inference, a lightweight predictor estimates query-conditioned mixture weights to synthesize a guidance vector entirely from these stored prototypes, eliminating the need for reference input. Second, to bridge the domain gap and effectively apply this synthesized guidance, we introduce a bidirectional alignment module that performs coupled attention between the synthesized guidance and query features to obtain a spatial gate, then applies the spatial modulation and a class-token offset to adapt both the query features and the class representation. Integrated into a modern COD backbone, this design provides flexible deployment and robust feature alignment.

Extensive experiments on the large-scale R2C7K benchmark and four standard COD datasets demonstrate the effectiveness and generalization of our framework. Under the standard Ref-COD protocol, our model achieves new state-of-the-art results across both CNN and Transformer backbones, even without test-time references. These results validate that our design preserves the semantic benefits of reference guidance while removing its practical constraints.

To summarize, our contributions are three-fold:

We address the core deployment paradox of Ref-COD.
 We propose RefOnce, the first framework to achieve fully reference-free inference, eliminating the impractical test-

- time dependency on reference images that hindered prior real-world application.
- To enable this paradigm, we design an efficient system that distills reference knowledge into a class-prototype memory and synthesizes adaptive guidance via a queryconditioned mixture mechanism. This system is complemented by a bidirectional attention alignment (BAA) module to effectively bridge the salient-to-camouflage domain gap.
- Extensive experiments demonstrate that RefOnce, despite requiring no test-time references, achieves new state-ofthe-art performance on the large-scale R2C7K benchmark. Crucially, our design provides strong generalization to unseen categories, a capability fundamentally unavailable to previous reference-dependent methods.

2. Related Work

2.1. Camouflaged Object Detection

Camouflaged Object Detection (COD) targets the segmentation of objects that deliberately mimic their surroundings, where extremely low contrast, background clutter, and subtle boundaries jointly impede reliable detection. COD has accelerated with standardized datasets/baselines that consolidated evaluation and training practice [5, 8, 30, 31, 35, 54]. Architecturally, transformer-driven and multi-scale designs enhance global-to-local reasoning and fine details, such as CamoFormer [51], ZoomNe(X)ts [34, 35], Feature-Shrinkage Pyramid [16], MSCAF [27], and FAPNet [59]. Boundary- and structure-aware modeling improves edge fidelity via explicit boundary decoders and reconstruction [12, 17, 38, 50, 60], complemented by texture/structure enhancement [1, 22, 54, 61]. Robustness is further advanced by uncertainty reasoning [21, 24, 49], iterative refinement [15, 19], and graph interaction [52, 53] to focus on ambiguous regions and hard pixels. Frequency- and texturedomain cues provide complementary signals for separating foreground from clutter (e.g., [12, 23, 39, 55, 58]). Depth cues further provide geometric priors that help distinguish camouflaged objects from visually similar backgrounds by revealing subtle spatial discontinuities [41, 42, 46]. More works can be found in recent surveys [9, 47, 57].

Despite these advances, COD still struggles with extremely low contrast, tiny targets, and cross-domain generalization [8, 31]. These limitations motivate Referring COD, which introduces explicit category-conditioned guidance from a few reference images to reduce ambiguity in low-contrast and small-object cases (e.g., [44, 56]).

2.2. Referring Camouflaged Object Detection

Referring Camouflaged Object Detection (Ref-COD) aims to segment the camouflaged target specified by a few reference images from the same category, leveraging the refer-

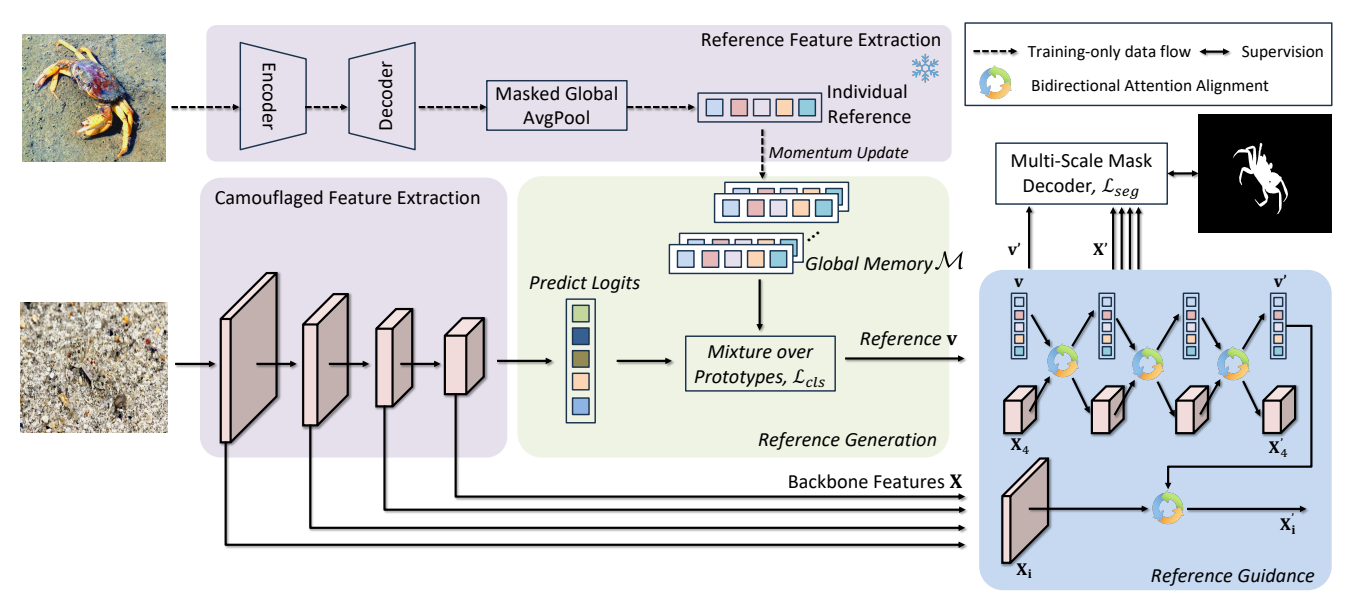


Figure 2. **Pipeline of the proposed RefOnce framework.** During training, the reference branch (top, dashed) distills features into a Global Memory \mathcal{M} ; at inference, the reference \mathbf{v} is synthesized from \mathcal{M} and predict logits.

ence images as category-consistent guidance for the query image. This task is motivated by the need to inject stable class-level cues for reliable detection in low-contrast and cluttered scenes. The seminal work R2CNet [56] introduced a simple solution which employs a dual-branch design to extract the high-level target features from reference images and guide the camouflaged branch to recognize the camouflaged objects. Subsequently, UAT [44] proposed an uncertainty-aware transformer that integrates reference semantics into camouflaged feature learning via a cross-attention encoder and models token-level dependencies as Gaussian random variables through a probabilistic decoder. RPMA [26] introduced an adapter that injects the reference cues to the transformer backbone with reference-generated dynamic convolutions.

However, these approaches still face two key limitations. First, they require reference images during inference, which restricts practical deployment since obtaining suitable references for each query is costly and often infeasible. Second, the salient-camouflage domain gap is insufficiently addressed, as global modulation or cross-attention from reference features often causes misalignment or over-transfer. To overcome these issues, we propose RefOnce, which distills reference knowledge into a class-prototype memory during training and performs reference-free inference with a bidirectional alignment module for robust feature adaptation.

3. Methodology

In this section, we will first summarize the overall architecture in Sec. 3.1. Then, we will introduce the class-prototype memory and the bidirectional alignment in Sec. 3.2 and

Sec. 3.3, respectively.

3.1. Architecture

Preliminary. Ref-COD is an emerging task, which detects and segments the camouflaged objects within a natural image via the specific guidance of the reference images with clear targets in the same categories. Given the input camouflaged image I and the reference image I_{ref} from the same category, the Ref-COD framework processes them separately via camouflaged and reference branches, and derives the multi-scale query features $\{X_i\}$ and a reference vector \mathbf{r} . With a guidance vector \mathbf{v} obtained from \mathbf{r} during training and synthesized from the prototype memory \mathcal{M} at inference, the query branch performs reference guidance on $\{X_i\}$, and the mask decoder predicts the binary mask M.

Feature extraction. Our method follows the above basic framework. The overall architecture of our method is illustrated in Fig. 2. It consists of five parts: reference feature generation, camouflage feature extraction, class-prototype memory generation, reference guidance, and multi-scale mask decoder. For convenience, we take ResNet-50 backbone [13] as the example. Given the camouflaged image I, the backbone network will extract it to four-stage features as X_1 , X_2 , X_3 , and X_4 , with strides of 4, 8, 16, 32, respectively. For the reference image I_{ref} , we employ the frozen ICON [62] network to extract the final saliency prediction features, followed by a multiplication of the foreground mask of the reference target. Then we conduct a global average pooling over each channel to derive the 1-D reference vector **r**. We then perform reference guidance on the multi-stage features X_i ($i \in [1,4]$) together with a guidance vector \mathbf{v} ; in our reference-free instantiation, \mathbf{v} is synthesized from the prototype memory at inference.

Reference generation and guidance. We decouple learning from inference: during training, the model summarizes category cues from references into a compact prototype memory \mathcal{M} ; at inference, given only a camouflaged query, a lightweight predictor consults this memory to produce a query-conditioned guidance vector \mathbf{v} , so no reference image or branch is required at test time. To make the guidance effective in low-contrast, cluttered scenes, we further apply a bidirectional alignment module that jointly adapts the query features and the guidance representation, and inject the guidance across multiple feature scales to highlight object-related regions while suppressing distractors. The specific designs of the prototype memory and the alignment will be detailed in Sec. 3.2 and Sec. 3.3.

Mask prediction. Given the aligned multi-scale features $\{X_i'\}$, we use a standard multi-scale mask decoder to predict the segmentation. In the regular instantiation, we first obtain a relevance seed by correlating the guidance vector with the top-stage refined feature map, and then inject this seed into a top-down mask decoder with progressive upsampling and lateral aggregation. For simplicity, we apply the mask decoder of ZoomNet [34] as our basic mask decoder.

Loss function. We supervise the model with two terms: (1) a binary cross-entropy (BCE) loss \mathcal{L}_{seg} on the predicted segmentation masks; (2) a token/classification loss \mathcal{L}_{cls} (Sec. 3.2) that supervises the mixture predictor for synthesizing \mathbf{v} from the memory. The final objective is $\mathcal{L} = \mathcal{L}_{\text{seg}} + \lambda_c \, \mathcal{L}_{\text{cls}}$, where $\lambda_c = 0.03$ in implementation.

3.2. Reference Generation

Prior Ref-COD frameworks [44, 56] adopt a reference-conditioned dual-branch design at test time, which leads to a core limitation: the dependency on reference images during inference. Fetching and encoding references increases latency and causes unstable guidance, as model behavior depends on which specific reference set is available. To eliminate this test-time dependency, we distill the category-level semantics of references into a prototype memory during training, which can be efficiently queried at inference to achieve reference-free, category-aware detection.

Let $\mathcal{M} = \{\mathbf{m}_1, \dots, \mathbf{m}_K\}$ be a learnable prototype memory (where K is the number of prototypes, typically the number of categories). Each prototype $\mathbf{m}_k \in \mathbb{R}^C$ encodes the global statistics of category k. It amortizes perimage reference vectors \mathbf{r} by aggregating their information into persistent, category-level prototypes. Given a reference vector $\mathbf{r} \in \mathbb{R}^C$ for category y, we update the memory with an exponential moving average (EMA):

$$\mathbf{m}_y \leftarrow \mu \, \mathbf{m}_y + (1 - \mu) \, \mathbf{r}, \quad 0 < \mu < 1,$$
 (1)

where μ is the momentum coefficient. At inference, given

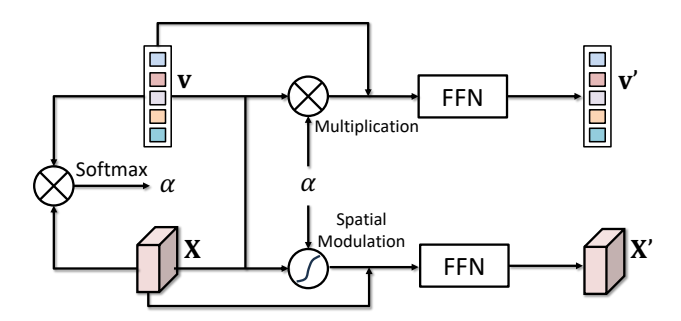


Figure 3. Architecture of the bidirectional attention alignment.

only a camouflaged query, we extract a compact descriptor $\mathbf{q} \in \mathbb{R}^C$ from the query features and predict logits $\mathbf{a} = h(\mathbf{q}) \in \mathbb{R}^K$. We then form a mixture over prototypes:

$$\pi = \operatorname{softmax}(\mathbf{a}),$$

$$\mathbf{v} = \sum_{k=1}^{K} \pi_k \, \mathbf{m}_k.$$
(2)

The vector $\mathbf{v} \in \mathbb{R}^C$ serves as the reference guidance synthesized without any test-time references.

During training, when a reference of category y is available, we encourage the predictor $h(\cdot)$ to produce category-consistent mixtures via a token/classification loss implemented by a standard cross-entropy loss:

$$\mathcal{L}_{\text{cls}} = -\log \frac{\exp(a_y)}{\sum_{j=1}^K \exp(a_j)}.$$
 (3)

Optionally, to bootstrap early learning, the synthesized guidance can be combined with the current reference token, e.g., $\tilde{\mathbf{v}} = \mathbf{v} + \mathbf{r}$ when the reference is present; at inference we use \mathbf{v} alone. The memory update uses stop-gradient to avoid collapsing to trivial solutions, while the predictor $h(\cdot)$ is trained with the token loss \mathcal{L}_{cls} .

The above mixture-based retrieval provides a soft, query-adaptive combination of prototypes that better handles intra-class diversity than nearest-prototype selection. Compared with test-time references, the class-prototype memory offers a stable prior with negligible overhead and no reference data collection in inference.

3.3. Bidirectional Attention Alignment

Even with a category-aware vector synthesized from the prototype memory, effectively transferring this guidance to the camouflaged query remains a significant challenge. As highlighted in the introduction, there exists a significant gap between the high-contrast, salient reference domain and the low-contrast, cluttered camouflaged query domain. Prior methods relying on simple global affine modulation often fail because they only weakly align spatial semantics, leading to over-transfer or misalignment. We therefore introduce a bidirectional attention alignment (BAA) mechanism

that allows mutual interaction between the query features and the reference guidance, so that the reference vector is dynamically refined by the most discriminative query regions. The architecture is illustrated in Fig. 3.

Let $\mathbf{X} \in \mathbb{R}^{C \times H \times W}$ be a query feature map and $\mathbf{v} \in \mathbb{R}^C$ the guidance. Flatten \mathbf{X} to $\mathbf{F} \in \mathbb{R}^{HW \times C}$ and compute coupled attention scores

$$s_{p} = \frac{\left\langle \text{LN}(\mathbf{F}_{p})\mathbf{W}_{x}, \text{LN}(\mathbf{v})\mathbf{W}_{v} \right\rangle}{\sqrt{C}}, \quad p = 1, \dots, HW$$

$$\alpha_{p} = \frac{\exp(s_{p})}{\sum_{t} \exp(s_{t})},$$
(4)

where LN is the LayerNorm. The spatial gate $\mathbf{G} \in \mathbb{R}^{1 \times H \times W}$ is the reshaped α . Conditioned on \mathbf{v} , we generate the scaling parameters as below:

$$\gamma = \tanh(\mathbf{W}_{\gamma}\mathbf{v}),
\beta = \tanh(\mathbf{W}_{\beta}\mathbf{v}),$$
(5)

and apply a spatially-adaptive modulation:

$$\mathbf{X}' = \mathbf{X} + \mathbf{G} \odot ((1+\gamma) \odot \mathbf{X} + \boldsymbol{\beta}), \tag{6}$$

where \odot is element-wise product with appropriate broadcasting, and 1 denotes an all-ones tensor of appropriate shape. In the reverse direction, we aggregate evidence from the image to refine the guidance:

$$\mathbf{c} = \sum_{p} \alpha_{p} \mathbf{W}_{c} \mathbf{F}_{p},$$

$$\Delta \mathbf{v} = \mathbf{W}_{o} \mathbf{c},$$

$$\mathbf{v}' = \mathbf{v} + \Delta \mathbf{v}.$$
(7)

We further stabilize both branches with residual feedforward updates:

$$\mathbf{v}' \leftarrow \mathbf{v}' + \text{FFN}(\text{LN}(\mathbf{v}'))$$

$$\mathbf{X}' \leftarrow \mathbf{X}' + \text{FFN}(\text{LN}(\mathbf{X}')),$$
(8)

where FFN is the feed-forward network with two linear layers and GELU [14] activation. \mathbf{v}' and \mathbf{X}' are refined reference vector and camouflaged features, respectively.

The whole process is iterable and we can run the above process for multiple times for better performance. Reference features are 1-d vectors which provide object-level guidance to camouflaged features, so we choose to run the above process three times on the high-level backbone features \mathbf{X}_4 while we only run once for other stage backbone features with the refined \mathbf{v}' as the reference.

4. Experiments

4.1. Setup

Datasets. We conduct our experiments primarily on the R2C7K dataset, a newly introduced benchmark comprising

6,615 samples across 64 categories. Each category contains 25 reference images, resulting in a total of 1,600 reference images. By default, we train each network on the training set of the R2C7K dataset. To further evaluate the generalization ability of our approach to conventional camouflage object detection (COD) scenarios, we also assess its performance on four widely used COD datasets: CAMO [20], CHAMELEON [37], COD10K [5], and NC4K [30]. Moreover, to rigorously test cross-category generalization, we curate an Unseen Classes dataset by selecting 596 images from these four datasets whose categories are not included among the 64 categories in R2C7K.

Evaluation metrics. We perform the benchmarks under the standard Ref-COD protocol. We report mean absolute error (MAE), structure-measure [3] (S_m), adaptive E-measure [4] (α E), and weighted F-measure [32] (wF): MAE (M) measures absolute difference to the ground truth; S_m captures region- and object-aware structural similarity; α E combines element-wise and image-level similarity; and wF integrates precision and recall with spatial weighting.

Implementation details. We implement our RefOnce via the PyTorch [36] framework. During training, we use the SGD (momentum 0.9, weight decay 5×10^{-4}) optimizer with initial learning rate of 0.05, linear warming up, and linear decay strategy. We train the network for 40 epochs with a batch size of 8. All images are resized to 384×384 . During training, we apply random crop, resize, and rotation as data augmentation. For each camouflaged query, we follow previous works [44, 56] to sample five same-category reference images and average the computed reference features into a single vector to condition the network during training. During inference, the network only relies on the class-prototype memory for camouflaged object references. The predictor $h(\cdot)$ is implemented by 2 linear layers and ReLU activation.

4.2. Results

Comparison with other state-of-the-arts. As shown in Table 1, our RefOnce consistently surpasses all recent RefCOD approaches under both CNN and transformer backbones. For CNN-based settings, RefOnce (ResNet-50) already outperforms representative reference-dependent models such as R2CNet [56], UAT [44], and RPMA [26], achieving higher accuracy without using any reference images at inference. Notably, RefOnce (PVTv2-B2) obtains the best performance with $S_m=0.890$ and $\alpha E=0.937$, establishing a new state-of-the-art on the R2C7K benchmark. These results demonstrate that our prototype memory and BAA effectively retain the semantic benefits of reference guidance while removing its inference-time dependency.

Qualitative comparison. Fig. 4 presents qualitative comparisons on R2C7K, where RefOnce produces more complete and precise object boundaries than prior meth-

Table 1. **Comparison with recent state-of-the-art methods**. The benchmark is performed on the R2C7K test set. Methods marked with ¹ and ² use the ZoomNet [34] and ZoomNeXt [35] mask decoders, respectively.

Models	Backbone	Overall				Single-obj			Multi-obj				
Stekeone Stekeone		$\overline{S_m\uparrow}$	α E \uparrow	w F \uparrow	M↓	$S_m \uparrow$	α E \uparrow	w F \uparrow	M↓	$S_m \uparrow$	α E \uparrow	w F \uparrow	M↓
CNN-based backb	CNN-based backbones												
PFNet-Ref [33]	ResNet-50 [13]	0.811	0.885	0.687	0.036	0.815	0.886	0.691	0.035	0.764	0.873	0.632	0.045
PreyNet-Ref [54]	ResNet-50 [13]	0.817	0.900	0.704	0.032	0.822	0.900	0.709	0.032	0.763	0.898	0.645	0.041
SINetV2-Ref [8]	Res2Net-50 [10]	0.823	0.888	0.700	0.033	0.828	0.889	0.705	0.032	0.771	0.874	0.634	0.043
BSANet-Ref [60]	Res2Net-50 [10]	0.830	0.912	0.727	0.030	0.827	0.913	0.733	0.030	0.774	0.895	0.655	0.039
BGNet-Ref [38]	Res2Net-50 [10]	0.840	0.909	0.738	0.029	0.844	0.910	0.742	0.029	0.792	0.887	0.679	0.036
DGNet-Ref [18]	EfficientNet-B4 [40]	0.821	0.891	0.696	0.032	0.827	0.890	0.703	0.031	0.748	0.879	0.607	0.045
UAT [44]	Res2Net-50 [10]	0.825	0.886	0.698	0.033	0.829	0.884	0.702	0.032	0.762	0.862	0.613	0.044
R2CNet1 [56]	ResNet-50 [13]	0.834	0.886	0.720	0.029	0.839	0.887	0.726	0.029	0.781	0.876	0.652	0.038
R2CNet ² [56]	ResNet-50 [13]	0.850	0.909	0.755	0.027	0.859	0.910	0.762	0.026	0.788	0.892	0.675	0.037
RefOnce ¹ (Ours)	ResNet-50 [13]	0.846	0.904	0.743	0.027	0.851	0.905	0.749	0.027	0.799	0.893	0.684	0.035
RefOnce ² (Ours)	ResNet-50 [13]	0.860	0.914	0.768	0.025	0.865	0.916	0.775	0.024	0.811	0.897	0.705	0.033
Transformer-base	d backbones												
VSCode-Ref [29]	Swin-S [28]	0.832	0.891	0.714	0.030	0.838	0.892	0.718	0.029	0.766	0.880	0.662	0.041
CIRCOD [11]	PVTv2-B2 [43]	0.848	0.918	0.756	0.026	-	-	-	-	-	-	-	-
UAT [44]	PVTv2-B2 [43]	0.855	0.912	0.757	0.026	0.859	0.913	0.761	0.025	0.805	0.900	0.701	0.033
RPMA [26]	SegFormer-B4 [48]	0.862	0.930	0.784	0.023	0.867	0.934	0.791	0.023	0.806	0.894	0.718	0.033
RefOnce ² (Ours)	PVTv2-B2 [43]	0.890	0.937	0.819	0.019	0.894	0.937	0.825	0.018	0.853	0.930	0.767	0.024

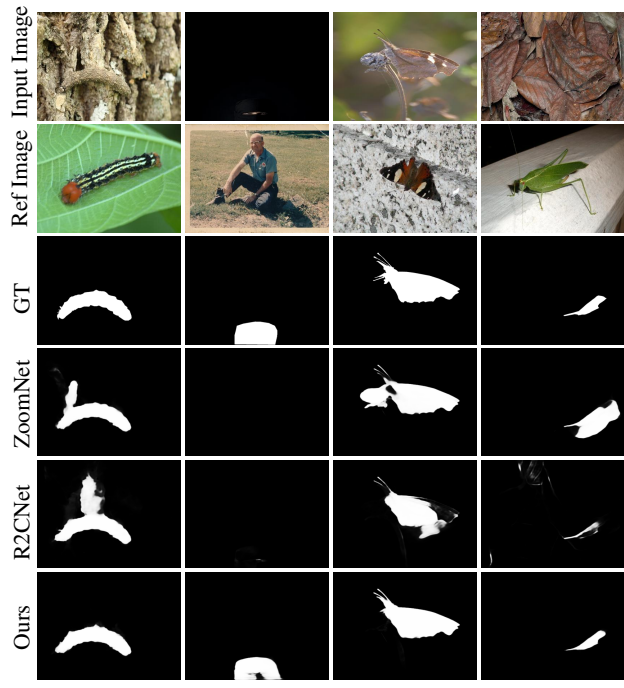


Figure 4. Qualitative comparison on R2C7K dataset.

ods. The masks generated by RefOnce are cleaner and better aligned with the concealed targets, especially in challenging low-light or cluttered scenes. For example, in the second example from the left, the human in a dark environment is barely detected by other models, while our approach correctly segments the entire figure. These visual results

confirm that RefOnce yields more reliable and fine-grained detection even without any test-time references.

4.3. Ablation Study

Significance of reference for COD. In this part, we analyze how reference information helps the network recognize camouflaged objects. COD is an inherently challenging task because the target often blends almost perfectly into the background, causing the backbone network to fail in capturing object-level semantics. As shown in Fig. 5, without any reference guidance (w/o Ref, column 4), the model's activation maps are scattered and mainly respond to background textures, indicating poor localization of the camouflaged object. Incorporating reference information provides strong semantic cues that help the model focus on the correct regions. The basic Ref-COD framework, R2C [56] (w/ R2C, column 5), partially alleviates this issue by introducing external guidance, yet the response remains inaccurate or incomplete due to weak feature alignment between reference and query. In contrast, our BAA-based approach (w/ BAA (Ours), column 6) effectively aligns the synthesized reference representation with the query features, enabling precise localization of the concealed target. Importantly, our model achieves this without requiring any reference image during inference, demonstrating that the distilled prototype memory and bidirectional alignment module allow the network to internalize reference cues and utilize them implicitly for more accurate and robust detection.

Generalization ability. To evaluate the generalization ability of our framework, we compare it with the baseline

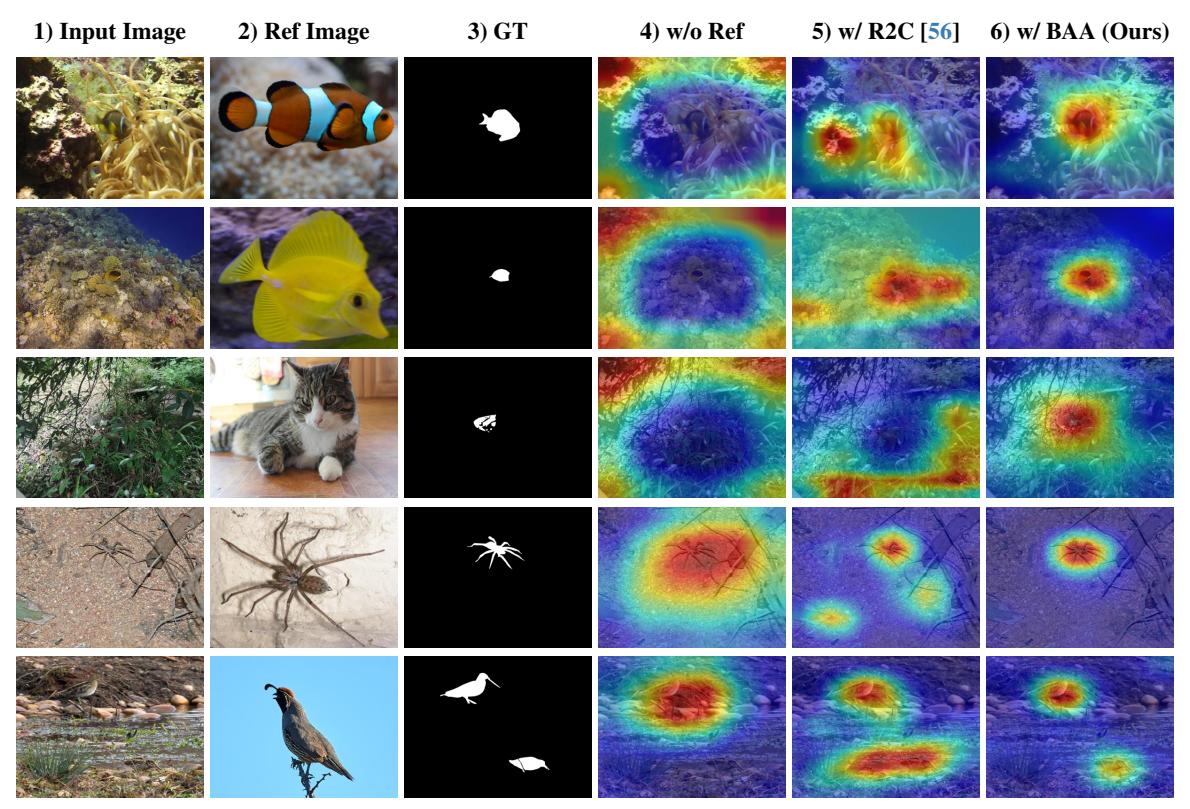


Figure 5. **Visualizations of backbone features with or without reference guidance**. "4) w/o Ref" indicates the visualization of backbone features before reference guidance. "5) w/ R2C" is the visualization of backbone features with R2C [56] as reference guidance. "6) w/ RefOnce (Ours)" replaces R2C with our BAA (Sec. 3.3) strategy. More examples can refer to the supplementary.

Table 2. Evaluation of the generalization ability of our RefOnce. The baseline is our method training without any reference guidance. Note that the performance gain (Δ) is most pronounced on the Unseen Classes subset, highlighting our model's strong generalization to novel categories.

Dataset	Method	$S_m \uparrow$	α E \uparrow	w F \uparrow	M↓
	Baseline (w/o Ref)	0.853	0.938	0.773	0.034
CHAMELEON	Ours	0.882	0.941	0.812	0.029
	Δ	+0.029	+0.003	+0.039	-0.005
	Baseline (w/o Ref)	0.698	0.794	0.564	0.108
CAMO	Ours	0.728	0.801	0.615	0.098
	Δ	+0.030	+0.007	+0.051	-0.010
	Baseline (w/o Ref)	0.817	0.881	0.695	0.033
COD10K	Ours	0.844	0.902	0.741	0.028
	Δ	+0.027	+0.021	+0.046	-0.005
	Baseline (w/o Ref)	0.824	0.890	0.744	0.052
NC4K	Ours	0.854	0.910	0.789	0.043
	Δ	+0.030	+0.020	+0.045	-0.009
	Baseline (w/o Ref)	0.801	0.868	0.713	0.061
Unseen Classes	Ours	0.839	0.892	0.770	0.048
	Δ	+0.038	+0.024	+0.057	-0.013

that removes the reference branch and trains the network without any reference guidance, while keeping other settings identical. Both the baseline and our method are trained on the R2C7K dataset. Results are shown in Table 2, which includes four standard COD benchmarks and one additional Unseen Classes subset. The Unseen Classes dataset is constructed from the above four COD benchmarks but deliberately excludes all categories contained in all classes of R2C7K. This setting aims to test the model's ability to generalize to novel categories never observed during training. We can observe that our model surpasses the baseline by a large margin in all datasets. Notably, the performance gain is most pronounced on the Unseen Classes subset (an S_m gain of +0.038, compared to \sim +0.027-0.030 on other datasets). This key finding highlights the baseline's vulnerability to novel categories, where its performance is weakest due to the lack of any relevant priors. In contrast, our model, by synthesizing a transferable semantic prior via the prototype mixture mechanism, provides the most significant relative advantage in this challenging scenario. This strongly suggests that the proposed prototype memory effectively captures transferable semantic priors, not just memorizing the training categories. This capability, combined with our model's reference-free inference, allows RefOnce to generalize smoothly to new categories, a task where previous reference-dependent methods fundamentally fail.

Table 3. Ablation study on the loss factor λ_c of \mathcal{L}_{cls} in generating the reference vector \mathbf{v} .

No.	λ_c	$S_m \uparrow$	$\alpha \mathrm{E} \uparrow$	w F \uparrow	M↓
1	0.3	0.794	0.856	0.650	0.037
2	0.1	0.830	0.886	0.713	0.030
3	0.03	0.846	0.904	0.743	0.027
4	0.01	0.838	0.893	0.730	0.029
5	0.003	0.835	0.896	0.730	0.029

Table 4. Ablation study on the momentum μ of updating the memory \mathcal{M} .

No.	μ	$S_m \uparrow$	αE↑	w F \uparrow	M↓
1	0.9	0.844	0.904	0.742	0.028
2	0.99	0.846	0.904	0.743	0.027
3	0.999	0.844	0.901	0.739	0.027

Momentum updates. As shown in Table 4, varying the momentum coefficient μ used for updating the prototype memory slightly affects the performance. The model achieves the best overall balance when $\mu=0.99$, indicating that a relatively slow update helps maintain stable category representations while still allowing gradual adaptation. Therefore, we adopt $\mu=0.99$ as the default setting.

Loss factor. As presented in Table 3, the weight λ_c of the classification loss significantly affects the performance. A moderate value of λ_c yields the best results, suggesting that an appropriate supervision strength effectively guides the mixture predictor without over-constraining it. Based on the results, we choose $\lambda_c = 0.03$ as the default setting.

Mixture over prototypes. To investigate the effect of synthesizing the reference vector, we compare two strategies: (1) mixture over prototypes, which forms a soft combination of all category prototypes using query-conditioned mixture weights; (2) select the nearest one, which simply selects the prototype corresponding to the largest predicted logit; (3) use the GT class, an upper-bound case where the ground-truth category of each query is provided during inference. As shown in Table 5, the mixture-based strategy consistently improves all metrics over the nearestprototype selection and approaches the upper-bound performance. These results demonstrate that soft combination over prototypes yields a more stable and informative reference representation, effectively approximating the ideal class-specific guidance without requiring any ground-truth information at test time.

BAA. Here we compare the BAA with the traditional one-way global modulation, which removes the inverse direction of refining the reference features in BAA. We observe that removing this direction in BAA results in a degradation of 0.4% S_m, 0.9% α E, 1.0% wF, and 0.1% MAE. This confirms that the reverse alignment, which allows the

Table 5. **Effect of mixture over prototypes**. We additionally report the upper-bound performance when the ground-truth class is provided during inference (Use the GT Class).

Setting	$S_m \uparrow$	α E \uparrow	w F \uparrow	M↓
Select the Nearest One	0.840	0.894	0.731	0.028
Mixture over Prototypes	0.846	0.904	0.743	0.027
Oracle: Use the GT Class	0.851	0.904	0.751	0.026

Table 6. **Computational cost analysis of RefOnce**. Gray texts indicate modules that are omitted during inference.

Module	# Params (M)	FLOPs (G)
Reference Feature Extraction	33.1	124.5
Reference Generation	0.1	0.01
Reference Guidance	2.5	13.7
Other parts	32.5	102.0

guidance vector to be refined by image-specific features, is crucial for effective feature adaptation and bridging the domain gap.

Computational overhead. We analyze the computational cost of our RefOnce, as shown in Table 6. We report the FLOPs and parameter counts of each major component, including reference feature extraction, reference generation, reference guidance, and the remaining parts (camouflaged feature extraction and mask prediction). During inference, the reference feature extraction module is omitted since RefOnce is reference-free. As shown in the table, this module accounts for a substantial portion of the total cost, comparable to the rest of the network. In contrast, reference generation is lightweight, requiring only 0.01 GFLOPs, and the reference guidance introduces an 11.8% overhead compared with the whole model during inference.

5. Conclusion

In this work, we introduced RefOnce, a reference-free framework for referring camouflaged object detection (Ref-COD). Unlike existing methods that require reference images during inference, RefOnce distills category-level semantics into a class-prototype memory and synthesizes query-conditioned guidance via a mixture over prototypes. A bidirectional attention alignment module further bridges the salient-camouflage domain gap by jointly adapting query features and class representations. Extensive experiments on the large-scale R2C7K benchmark and multiple standard COD datasets demonstrate that our approach achieves new state-of-the-art performance and exhibits strong generalization to unseen categories, even without any test-time references. We believe RefOnce provides a promising step toward deployable reference-guided segmentation without dependency on external examples.

References

- [1] Tianyou Chen, Jin Xiao, Xiaoguang Hu, Guofeng Zhang, and Shaojie Wang. Boundary-guided network for camouflaged object detection. *Knowledge-Based Systems*, 248: 108901, 2022. 2
- [2] Hung-Kuo Chu, Wei-Hsin Hsu, Niloy J Mitra, Daniel Cohen-Or, Tien-Tsin Wong, and Tong-Yee Lee. Camouflage images. ACM Trans. Graph. (TOG), 29(4):51–1, 2010.
- [3] Deng-Ping Fan, Ming-Ming Cheng, Yun Liu, Tao Li, and Ali Borji. Structure-measure: A new way to evaluate foreground maps. In *Int. Conf. Comput. Vis. (ICCV)*, pages 4548–4557, 2017. 5
- [4] Deng-Ping Fan, Cheng Gong, Yang Cao, Bo Ren, Ming-Ming Cheng, and Ali Borji. Enhanced-alignment measure for binary foreground map evaluation. In *Int. Joint Conf. Artif. Intell. (IJCAI)*, pages 698–704, 2018. 5
- [5] Deng-Ping Fan, Ge-Peng Ji, Guolei Sun, Ming-Ming Cheng, Jianbing Shen, and Ling Shao. Camouflaged object detection. In *IEEE Conf. Comput. Vis. Pattern Recog. (CVPR)*, pages 2777–2787, 2020. 1, 2, 5
- [6] Deng-Ping Fan, Ge-Peng Ji, Tao Zhou, Geng Chen, Huazhu Fu, Jianbing Shen, and Ling Shao. Pranet: Parallel reverse attention network for polyp segmentation. In *Med. Image Comput. Comput.-Assist. Interv. (MICCAI)*, pages 263–273. Springer, 2020. 1
- [7] Deng-Ping Fan, Tao Zhou, Ge-Peng Ji, Yi Zhou, Geng Chen, Huazhu Fu, Jianbing Shen, and Ling Shao. Inf-net: Automatic covid-19 lung infection segmentation from ct images. *IEEE Trans. Med. Imaging (TMI)*, 39(8):2626–2637, 2020.
- [8] Deng-Ping Fan, Ge-Peng Ji, Ming-Ming Cheng, and Ling Shao. Concealed object detection. *IEEE Trans. Pattern Anal. Mach. Intell. (TPAMI)*, 44(10):6024–6042, 2021. 1, 2, 6
- [9] Deng-Ping Fan, Ge-Peng Ji, Peng Xu, Ming-Ming Cheng, Christos Sakaridis, and Luc Van Gool. Advances in deep concealed scene understanding. *Visual Intelligence*, 1(1):16, 2023. 2
- [10] Shang-Hua Gao, Ming-Ming Cheng, Kai Zhao, Xin-Yu Zhang, Ming-Hsuan Yang, and Philip Torr. Res2net: A new multi-scale backbone architecture. *IEEE Trans. Pattern Anal. Mach. Intell. (TPAMI)*, 43(2):652–662, 2019. 6
- [11] Avi Gupta, Koteswar Rao Jerripothula, and Tammam Tillo. Circod: Co-saliency inspired referring camouflaged object discovery. In *IEEE Winter Conf. Appl. Comput. Vis. (WACV)*, pages 8302–8312, 2025. 6
- [12] Chunming He, Kai Li, Yachao Zhang, Longxiang Tang, Yulun Zhang, Zhenhua Guo, and Xiu Li. Camouflaged object detection with feature decomposition and edge reconstruction. In *IEEE Conf. Comput. Vis. Pattern Recog. (CVPR)*, pages 22046–22055, 2023. 2
- [13] Kaiming He, Xiangyu Zhang, Shaoqing Ren, and Jian Sun. Deep residual learning for image recognition. In *IEEE Conf. Comput. Vis. Pattern Recog. (CVPR)*, pages 770–778, 2016. 3, 6
- [14] Dan Hendrycks and Kevin Gimpel. Gaussian error linear units (gelus). *arXiv preprint arXiv:1606.08415*, 2016. 5

- [15] Xiaobin Hu, Shuo Wang, Xuebin Qin, Hang Dai, Wenqi Ren, Donghao Luo, Ying Tai, and Ling Shao. High-resolution iterative feedback network for camouflaged object detection. In AAAI Conf. Artif. Intell. (AAAI), pages 881–889, 2023. 2
- [16] Zhou Huang, Hang Dai, Tian-Zhu Xiang, Shuo Wang, Huai-Xin Chen, Jie Qin, and Huan Xiong. Feature shrinkage pyramid for camouflaged object detection with transformers. In *IEEE Conf. Comput. Vis. Pattern Recog. (CVPR)*, pages 5557–5566, 2023. 2
- [17] Ge-Peng Ji, Lei Zhu, Mingchen Zhuge, and Keren Fu. Fast camouflaged object detection via edge-based reversible recalibration network. *Pattern Recognition (PR)*, 123:108414, 2022. 2
- [18] Ge-Peng Ji, Deng-Ping Fan, Yu-Cheng Chou, Dengxin Dai, Alexander Liniger, and Luc Van Gool. Deep gradient learning for efficient camouflaged object detection. *Machine Intelligence Research (MIR)*, 20(1):92–108, 2023. 6
- [19] Qi Jia, Shuilian Yao, Yu Liu, Xin Fan, Risheng Liu, and Zhongxuan Luo. Segment, magnify and reiterate: Detecting camouflaged objects the hard way. In *IEEE Conf. Comput.* Vis. Pattern Recog. (CVPR), pages 4713–4722, 2022. 2
- [20] Trung-Nghia Le, Tam V Nguyen, Zhongliang Nie, Minh-Triet Tran, and Akihiro Sugimoto. Anabranch network for camouflaged object segmentation. *Comput. Vis. Image Underst. (CVIU)*, 184:45–56, 2019. 5
- [21] Aixuan Li, Jing Zhang, Yunqiu Lv, Bowen Liu, Tong Zhang, and Yuchao Dai. Uncertainty-aware joint salient object and camouflaged object detection. In *IEEE Conf. Comput. Vis. Pattern Recog. (CVPR)*, pages 10071–10081, 2021. 2
- [22] Peng Li, Xuefeng Yan, Hongwei Zhu, Mingqiang Wei, Xiao-Ping Zhang, and Jing Qin. Findnet: Can you find me? boundary-and-texture enhancement network for camouflaged object detection. *IEEE Trans. Image Process. (TIP)*, 31:6396–6411, 2022. 2
- [23] Jiaying Lin, Xin Tan, Ke Xu, Lizhuang Ma, and Rynson WH Lau. Frequency-aware camouflaged object detection. ACM Trans. Multimedia Comput. Commun. Appl., 19(2):1–16, 2023. 2
- [24] Jiawei Liu, Jing Zhang, and Nick Barnes. Modeling aleatoric uncertainty for camouflaged object detection. In *IEEE Winter Conf. Appl. Comput. Vis.* (WACV), pages 1445–1454, 2022. 2
- [25] Liu Liu, Rujing Wang, Chengjun Xie, Po Yang, Fangyuan Wang, Sud Sudirman, and Wancai Liu. Pestnet: An end-toend deep learning approach for large-scale multi-class pest detection and classification. *IEEE Access*, 7:45301–45312, 2019. 1
- [26] Xuewei Liu, Shaofei Huang, Ruipu Wu, Hengyuan Zhao, Duo Xu, Xiaoming Wei, Jizhong Han, and Si Liu. Reference prompted model adaptation for referring camouflaged object detection. In *Int. Conf. Multimedia and Expo (ICME)*, pages 1–6. IEEE, 2024. 3, 5, 6
- [27] Yu Liu, Haihang Li, Juan Cheng, and Xun Chen. Mscafnet: a general framework for camouflaged object detection via learning multi-scale context-aware features. *IEEE Trans. Circuit Syst. Video Technol. (TCSVT)*, 2023. 2
- [28] Ze Liu, Yutong Lin, Yue Cao, Han Hu, Yixuan Wei, Zheng Zhang, Stephen Lin, and Baining Guo. Swin transformer:

- Hierarchical vision transformer using shifted windows. In *Int. Conf. Comput. Vis. (ICCV)*, pages 10012–10022, 2021.
- [29] Ziyang Luo, Nian Liu, Wangbo Zhao, Xuguang Yang, Dingwen Zhang, Deng-Ping Fan, Fahad Khan, and Junwei Han. Vscode: General visual salient and camouflaged object detection with 2d prompt learning. In *IEEE Conf. Comput. Vis. Pattern Recog. (CVPR)*, pages 17169–17180, 2024. 6
- [30] Yunqiu Lv, Jing Zhang, Yuchao Dai, Aixuan Li, Bowen Liu, Nick Barnes, and Deng-Ping Fan. Simultaneously localize, segment and rank the camouflaged objects. In *IEEE Conf. Comput. Vis. Pattern Recog. (CVPR)*, pages 11591–11601, 2021. 2, 5
- [31] Yunqiu Lv, Jing Zhang, Yuchao Dai, Aixuan Li, Nick Barnes, and Deng-Ping Fan. Towards deeper understanding of camouflaged object detection. *IEEE Trans. Circuit Syst. Video Technol. (TCSVT)*, 2023. 1, 2
- [32] Ran Margolin, Lihi Zelnik-Manor, and Ayellet Tal. How to evaluate foreground maps? In *IEEE Conf. Comput. Vis. Pat*tern Recog. (CVPR), pages 248–255, 2014. 5
- [33] Haiyang Mei, Ge-Peng Ji, Ziqi Wei, Xin Yang, Xiaopeng Wei, and Deng-Ping Fan. Camouflaged object segmentation with distraction mining. In *IEEE Conf. Comput. Vis. Pattern Recog. (CVPR)*, pages 8772–8781, 2021. 6
- [34] Youwei Pang, Xiaoqi Zhao, Tian-Zhu Xiang, Lihe Zhang, and Huchuan Lu. Zoom in and out: A mixed-scale triplet network for camouflaged object detection. In *IEEE Conf. Com*put. Vis. Pattern Recog. (CVPR), pages 2160–2170, 2022. 2, 4, 6
- [35] Youwei Pang, Xiaoqi Zhao, Tian-Zhu Xiang, Lihe Zhang, and Huchuan Lu. ZoomNeXt: A unified collaborative pyramid network for camouflaged object detection. *IEEE Trans. Pattern Anal. Mach. Intell. (TPAMI)*, 46(12):9205–9220, 2024. 1, 2, 6
- [36] Adam Paszke, Sam Gross, Francisco Massa, Adam Lerer, James Bradbury, Gregory Chanan, Trevor Killeen, Zeming Lin, Natalia Gimelshein, Luca Antiga, et al. Pytorch: An imperative style, high-performance deep learning library. Adv. Neural Inform. Process. Syst. (NeurIPS), 32, 2019. 5
- [37] Przemysław Skurowski, Hassan Abdulameer, Jakub Błaszczyk, Tomasz Depta, Adam Kornacki, and Przemysław Kozieł. Animal camouflage analysis: Chameleon database. *Unpublished manuscript*, 2(6):7, 2018. 5
- [38] Yujia Sun, Shuo Wang, Chenglizhao Chen, and Tian-Zhu Xiang. Boundary-guided camouflaged object detection. In Int. Joint Conf. Artif. Intell. (IJCAI), pages 1335–1341, 2022. 2, 6
- [39] Yanguang Sun, Chunyan Xu, Jian Yang, Hanyu Xuan, and Lei Luo. Frequency-spatial entanglement learning for camouflaged object detection. In *Eur. Conf. Comput. Vis.* (*ECCV*), pages 343–360, 2024. 2
- [40] Mingxing Tan and Quoc Le. Efficientnet: Rethinking model scaling for convolutional neural networks. In *Int. Conf. Mach. Learn. (ICML)*, pages 6105–6114. PMLR, 2019. 6
- [41] Liqiong Wang, Jinyu Yang, Yanfu Zhang, Fangyi Wang, and Feng Zheng. Depth-aware concealed crop detection in dense agricultural scenes. In *IEEE Conf. Comput. Vis. Pattern Recog. (CVPR)*, pages 17201–17211, 2024. 2

- [42] Qingwei Wang, Jinyu Yang, Xiaosheng Yu, Fangyi Wang, Peng Chen, and Feng Zheng. Depth-aided camouflaged object detection. In ACM Int. Conf. Multimedia (ACM MM), pages 3297–3306, 2023. 2
- [43] Wenhai Wang, Enze Xie, Xiang Li, Deng-Ping Fan, Kaitao Song, Ding Liang, Tong Lu, Ping Luo, and Ling Shao. Pvt v2: Improved baselines with pyramid vision transformer. *Comput. Visual Media (CVMJ)*, 8(3):415–424, 2022. 6
- [44] Ranwan Wu, Tian-Zhu Xiang, Guo-Sen Xie, Rongrong Gao, Xiangbo Shu, Fang Zhao, and Ling Shao. Uncertaintyaware transformer for referring camouflaged object detection. *IEEE Trans. Image Process. (TIP)*, 2025. 1, 2, 3, 4, 5, 6
- [45] Yu-Huan Wu, Shang-Hua Gao, Jie Mei, Jun Xu, Deng-Ping Fan, Rong-Guo Zhang, and Ming-Ming Cheng. Jcs: An explainable covid-19 diagnosis system by joint classification and segmentation. *IEEE Trans. Image Process. (TIP)*, 30: 3113–3126, 2021. 1
- [46] Zongwei Wu, Danda Pani Paudel, Deng-Ping Fan, Jingjing Wang, Shuo Wang, Cédric Demonceaux, Radu Timofte, and Luc Van Gool. Source-free depth for object pop-out. In *Int. Conf. Comput. Vis. (ICCV)*, pages 1032–1042, 2023.
- [47] Fengyang Xiao, Sujie Hu, Yuqi Shen, Chengyu Fang, Jinfa Huang, Chunming He, Longxiang Tang, Ziyun Yang, and Xiu Li. A survey of camouflaged object detection and beyond. arXiv preprint arXiv:2408.14562, 2024. 2
- [48] Enze Xie, Wenhai Wang, Zhiding Yu, Anima Anandkumar, Jose M Alvarez, and Ping Luo. Segformer: Simple and efficient design for semantic segmentation with transformers. Adv. Neural Inform. Process. Syst. (NeurIPS), 34:12077– 12090, 2021. 6
- [49] Fan Yang, Qiang Zhai, Xin Li, Rui Huang, Ao Luo, Hong Cheng, and Deng-Ping Fan. Uncertainty-guided transformer reasoning for camouflaged object detection. In *Int. Conf. Comput. Vis. (ICCV)*, pages 4146–4155, 2021. 2
- [50] Sheng Ye, Xin Chen, Yan Zhang, Xianming Lin, and Liujuan Cao. Escnet: Edge-semantic collaborative network for camouflaged object detection. In *Int. Conf. Comput. Vis. (ICCV)*, pages 20053–20063, 2025. 2
- [51] Bowen Yin, Xuying Zhang, Deng-Ping Fan, Shaohui Jiao, Ming-Ming Cheng, Luc Van Gool, and Qibin Hou. Camoformer: Masked separable attention for camouflaged object detection. *IEEE Trans. Pattern Anal. Mach. Intell. (TPAMI)*, 2024. 2
- [52] Qiang Zhai, Xin Li, Fan Yang, Chenglizhao Chen, Hong Cheng, and Deng-Ping Fan. Mutual graph learning for camouflaged object detection. In *IEEE Conf. Comput. Vis. Pattern Recog. (CVPR)*, pages 12997–13007, 2021. 2
- [53] Qiang Zhai, Xin Li, Fan Yang, Zhicheng Jiao, Ping Luo, Hong Cheng, and Zicheng Liu. Mgl: Mutual graph learning for camouflaged object detection. *IEEE Trans. Image Process.*, 32:1897–1910, 2022. 2
- [54] Miao Zhang, Shuang Xu, Yongri Piao, Dongxiang Shi, Shusen Lin, and Huchuan Lu. Preynet: Preying on camouflaged objects. In *ACM Int. Conf. Multimedia (ACM MM)*, pages 5323–5332, 2022. 2, 6
- [55] Shizhou Zhang, Dexuan Kong, Yinghui Xing, Yue Lu, Lingyan Ran, Guoqiang Liang, Hexu Wang, and Yanning

- Zhang. Frequency-guided spatial adaptation for camouflaged object detection. *IEEE Trans. Multimedia (TMM)*, 27:72–83, 2025. 2
- [56] Xuying Zhang, Bowen Yin, Zheng Lin, Qibin Hou, Deng-Ping Fan, and Ming-Ming Cheng. Referring camouflaged object detection. *IEEE Trans. Pattern Anal. Mach. Intell.* (TPAMI), 2025. 1, 2, 3, 4, 5, 6, 7
- [57] Pancheng Zhao, Deng-Ping Fan, Shupeng Cheng, Salman Khan, Fahad Shahbaz Khan, David Clifton, Peng Xu, and Jufeng Yang. Deep learning in concealed dense prediction. *arXiv preprint arXiv:2504.10979*, 2025. 2
- [58] Yijie Zhong, Bo Li, Lv Tang, Senyun Kuang, Shuang Wu, and Shouhong Ding. Detecting camouflaged object in frequency domain. In *IEEE Conf. Comput. Vis. Pattern Recog.* (CVPR), pages 4504–4513, 2022. 2
- [59] Tao Zhou, Yi Zhou, Chen Gong, Jian Yang, and Yu Zhang. Feature aggregation and propagation network for camouflaged object detection. *IEEE Trans. Image Process. (TIP)*, 31:7036–7047, 2022. 2
- [60] Hongwei Zhu, Peng Li, Haoran Xie, Xuefeng Yan, Dong Liang, Dapeng Chen, Mingqiang Wei, and Jing Qin. I can find you! boundary-guided separated attention network for camouflaged object detection. In *AAAI Conf. Artif. Intell.* (*AAAI*), pages 3608–3616, 2022. 2, 6
- [61] Jinchao Zhu, Xiaoyu Zhang, Shuo Zhang, and Junnan Liu. Inferring camouflaged objects by texture-aware interactive guidance network. In AAAI Conf. Artif. Intell. (AAAI), 2021.
- [62] Mingchen Zhuge, Deng-Ping Fan, Nian Liu, Dingwen Zhang, Dong Xu, and Ling Shao. Salient object detection via integrity learning. *IEEE Trans. Pattern Anal. Mach. Intell. (TPAMI)*, 45(3):3738–3752, 2022. 3